Available online at www.sciencedirect.com

SCIENCE DIRECT

Developmental Biology 284 (2005) 523 – 535

DEVELOPMENTAL BIOLOGY

www.elsevier.com/locate/ydbio

Genomes & Developmental Control

Computational analysis of EGFR inhibition by Argos

Gregory T. Reeves[a,b], Rachel Kalifa[a,b], Daryl E. Klein[c], Mark A. Lemmon[c], Stanislav Y. Shvartsman[a,b,*]

[a]*Department of Chemical Engineering, Princeton University, Princeton, NJ 08544, USA*
[b]*Lewis-Sigler Institute for Integrative Genomics, Princeton University, Carl Icahn Laboratory, Washington Road, Princeton, NJ 08544, USA*
[c]*Department of Biochemistry and Biophysics, University of Pennsylvania School of Medicine, Philadelphia, PA 1904, USA*

Received for publication 17 January 2005, revised 2 May 2005, accepted 4 May 2005
Available online 27 June 2005

Abstract

Argos, a secreted inhibitor of the *Drosophila* epidermal growth factor receptor, and the only known secreted receptor tyrosine kinase inhibitor, acts by sequestering the EGFR ligand Spitz. We use computational modeling to show that this biochemically-determined mechanism of Argos action can explain available genetic data for EGFR/Spitz/Argos interactions in vivo. We find that efficient Spitz sequestration by Argos is key for explaining the existing data and for providing a robust feedback loop that modulates the Spitz gradient in embryonic ventral ectoderm patterning. Computational analysis of the EGFR/Spitz/Argos module in the ventral ectoderm shows that Argos need not be long-ranged to account for genetic data, and can actually have very short range. In our models, Argos with long or short length scale functions to limit the range and action of secreted Spitz. Thus, the spatial range of Argos does not have to be tightly regulated or may act at different ranges in distinct developmental contexts.

Keywords: EGFR inhibition; Argos; Spitz

Introduction

Epidermal growth factor receptor (EGFR) is a key regulator of developing tissues in animals from worms to humans (Holbro and Hynes, 2004; Moghal and Sternberg, 2003; Shilo, 2003). EGFR activation in vivo is tightly controlled by ligand availability, receptor-mediated endocytosis, and intracellular inhibitors of EGFR signaling (Harris et al., 2003; Sweeney and Carraway, 2004). Experiments in *Drosophila* have identified a secreted EGFR inhibitor, Argos, that participates in a negative feedback loop induced by high levels of EGFR signaling (Casci and Freeman, 1999; Freeman et al., 1992; Schweitzer et al., 1995a; Shilo, 2003). Genetic studies have demonstrated that EGFR inhibition by Argos is long-ranged in all stages of fruit fly development (Freeman et al., 1992). Recently, we have shown biochemically that Argos inhibits EGFR signaling by sequestering the activating ligand Spitz (Klein et al., 2004). This direct interaction of Argos and Spitz suggests that the apparent long-range of EGFR inhibition by Argos may result not from the long range of the molecule itself, but from its ability to modulate the gradients of secreted EGFR agonists such as Spitz (Klein et al., 2004). Sequestration of EGFR agonists by Argos could result in long-ranged EGFR inhibition in two different ways. First, by sequestering Spitz close to the point of its release and thus preventing Spitz delivery to distant cells, Argos could act as a short-ranged molecule with long-range effects. Second, Argos could diffuse to distant cells and inhibit EGFR signaling by sequestering activating ligands at a distance from the site of their secretion.

Experimental tests of the ability of Argos to directly modulate the gradients of locally produced EGFR ligands require visualizing these gradients in vivo. Currently, these

* Corresponding author. Lewis-Sigler Institute for Integrative Genomics, Princeton University, Carl Icahn Laboratory, Washington Road, Princeton, NJ 08544, USA. Fax: +1 609 258 3565.
E-mail address: stas@princeton.edu (S.Y. Shvartsman).

0012-1606/$ - see front matter © 2005 Elsevier Inc. All rights reserved.
doi:10.1016/j.ydbio.2005.05.013

gradients can only be followed indirectly, through analysis of signaling and transcriptional targets of EGFR. To investigate the spatiotemporal control of EGFR signaling by Argos, we have developed a computational model of the EGFR/Spitz/Argos network and used it to study the role of Argos in cell fate determination in the ventral ectoderm (Golembo et al., 1996a, b; Kim and Crews, 1993; Lee et al., 1999; Raz and Shilo, 1993).

In stage 5 of embryonic development, the cellularized blastoderm contains spatial information that divides the embryo along its dorsal–ventral axis into distinct domains, including the presumptive mesodermal, mesectodermal, and ventral ectodermal domains. The cells in the presumptive mesoderm, the ventral-most of these domains, invaginate during gastrulation in stages 6 and 7. This causes the two presumptive mesectodermal domains, each corresponding to a single row of cells on either side of the bilaterally symmetric embryo, to come together to form the ventral midline. After gastrulation is completed at stage 8, the cell row along the ventral midline is flanked on either side by the ventral ectoderm (VE). This cell row expresses the transcription factor *single-minded* (*sim*), which drives expression of the protease *rhomboid* (*rho*) ((Chang et al., 2001, 2003; Golembo et al., 1996a; Schweitzer et al., 1995b), Fig. 1B). Rhomboid is responsible for processing the EGFR ligand Spitz (Spi) into its active form (Lee et al., 2001). Secreted Spitz (sSpi) is thus produced only in the ventral midline, and diffuses to induce transcription of EGFR-target genes in the neighboring VE cells (Fig. 1A). These target genes fall into two distinct categories: the high-threshold genes, including *pointed* (*pnt*), *orthodenticle* (*otd*), and *argos* (*aos*), and the low-threshold genes such as *fasciclinIII* (*fasIII*). The high threshold genes are only expressed in the cells closest to the source of Spitz, where levels of the activating ligand are greatest: 1–2 cell rows on either side of the ventral midline (red arrow in Fig. 1A, (Chang et al., 2001, 2003; Golembo et al., 1996b; Vivekanand et al., 2004), Figs. 1C, D). Further from the ligand source, where Spitz levels are reduced, only

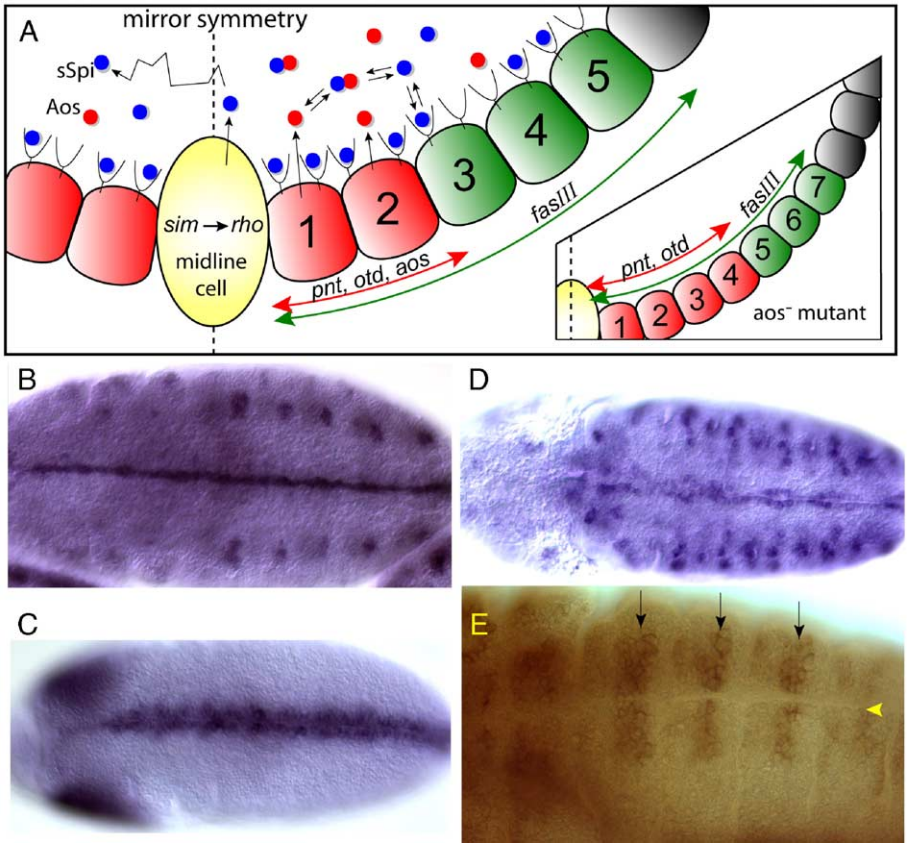

Fig. 1. Geometry of the ventral ectoderm. (A) EGFR-mediated cell communication in the ventral ectoderm. The midline cell is unique in that it expresses the transcription factor *sim*, which induces the expression of the protease Rhomboid. Rhomboid in turn processes the EGFR ligand Spitz, enabling Spitz to be secreted from the midline cell. Spitz diffuses in the extracellular space to neighboring ventral ectodermal cells, where it binds to and activates EGFR. As a consequence of EGFR activation, the first 1–2 rows of ventral ectoderm cells express the high threshold genes (*pnt*, *otd*, *aos*), as denoted by the red double-headed arrow. The low threshold genes (*fasIII*) are expressed in 4–5 cell rows (green double-headed arrow). The EGFR inhibitor Argos is secreted from the ventral-most 1–2 cell rows (as a high threshold gene product) and binds to Spitz in the extracellular space. In the Argos mutant, this inhibition is abolished, resulting in expansion of the expression domains of the high threshold genes to 3–6 cell rows, and the low threshold genes to 6–7 cell rows (see inset). (B–E) Visualization of expression domains of ventral ectoderm markers. (B) Rhomboid (*rho*) mRNA. (C) *otd* mRNA. (D) *aos* mRNA. (E) FasIII protein (arrows). Arrowhead: ventral midline.

the low threshold genes are expressed; this "low threshold" domain extends no more than 4–5 cell rows on either side of the midline (green arrow in Fig. 1A, (Chang et al., 2001, 2003; Golembo et al., 1996b; Patel et al., 1987; Vivekanand et al., 2004), Fig. 1E).

Argos appears to have two roles in VE patterning. First, it limits the lateral extent of Spitz signaling across the ventral ectoderm. Second, Argos is thought to provide a negative feedback loop that dampens fluctuations in other components of this signaling module, and thus contributes to the robustness of the wild-type expression pattern of EGFR target genes (Golembo et al., 1996a). The expression domains of EGFR-target genes are clearly expanded in *aos*$^-$ embryos compared to the wild-type case (Chang et al., 2001, 2003; Golembo et al., 1996a,b). The high-threshold domain expands from just 1–2 cell rows on either side of the midline (in wild type) to 3–6 cells on either side in *aos*$^-$ embryos (Chang et al., 2001, 2003; Golembo et al., 1996a,b) (red arrow in Fig. 1A, inset). Similarly, the low threshold domain expands from just 4–5 cell rows in wild type to 6–7 rows in the *aos*$^-$ mutants (Chang et al., 2001; Golembo et al., 1996a,b) (green arrow in Fig. 1A, inset). This expansion in the expression domains of EGFR target genes is accompanied by an increased width of the ventral epidermis, as measured by the distance between the precursors of the Keilin's organs, pairs of ventrolaterally located sensory organs (Freeman et al., 1992).

We have constrained our quantitative model of the EGFR/Spitz/Argos system in VE patterning using the experimentally observed expansions of EGFR-target gene expression in *aos*$^-$ embryos (Golembo et al., 1996b). After applying these constraints, we find that Argos can exert its influence on VE patterning by acting at very short range. Indeed, even when the Argos length scale is set to zero, the model can fit the experimental data obtained with *aos*$^-$ embryos. Our model also captures the experimentally observed robustness of the wild type signaling module to large changes in the doses of Spitz and EGFR (Golembo et al., 1996a, 1999; Raz and Shilo, 1993). We analyze the contribution of Argos to this robustness and show that it is not dependent on Argos being a long-ranged diffusible molecule: Argos can also achieve its stabilizing effects through short-range action.

Model of EGFR/Spitz/Argos network in the embryonic ventral ectoderm

Our model retains the essential interactions in the EGFR/Spitz/Argos network (Casci and Freeman, 1999; Chang et al., 2001, 2003; Golembo et al., 1996a,b, 1999; Klein et al., 2004; Schweitzer et al., 1995b; Shilo, 2003). We model Spitz diffusion and binding to EGFR, dimerization of Spitz/EGFR complexes, internalization of dimerized EGF receptors, as well as Argos binding to Spitz (which prevents Spitz from binding and activating EGFR). All of these interactions have been demonstrated either genetically or biochemically (Klein et al., 2004; Schweitzer et al., 1995b). In addition, Argos binds to the surface of *Drosophila* cells in culture through an interaction that can be inhibited by adding excess soluble heparin (Klein et al., 2004) and may possibly represent association with cell surface heparan-sulfate proteoglycans (HSPGs). To account for this, we include a term in our model that describes binding of Argos to the cell surface and assume that this represents one route for Argos uptake (and thus removal) in the ventral ectoderm, as reported for other such interactions (Colin et al., 1999; Deguchi et al., 2002).

The starting model of EGFR signaling in the ventral ectoderm has one intracellular, three cell-surface, and three extracellular variables (see Supplementary Material for the details of model formulation). The intracellular variable describes the level of an EGFR-regulated transcription factor in cell *i*. This variable lumps the joint effects of ETS transcriptional activators and repressors, such as Pointed and Yan, that convert EGFR-mediated MAPK signaling into the expression of high-threshold genes (Chang et al., 2001, 2003; Golembo et al., 1996a,b, 1999; Vivekanand et al., 2004). In the rest of the paper, we refer to this intracellular variable as "Pointed". The cell surface variables are the levels of Spitz/EGFR complexes, of cell surface-bound Argos, and of dimerized receptor. The extracellular variables represent the concentrations of diffusing Spitz, Argos, and the Argos/Spitz complex.

The input to the system is modeled as a localized and constant Spitz generation term that represents the activity of Rhomboid in the midline cell, which is required for processing and secretion of active Spitz. In contrast, EGFR is expressed only in the ventral ectodermal cells, and not in the midline (Raz and Shilo, 1993; Zak et al., 1990). The generation rate of the transcription factor that controls the expression of Argos in cell *i* is a function of the level of EGFR activity seen by cell *i*, which is taken as the total number of EGFR dimers. Pointed, expressed in response to high levels of EGFR activation, stimulates Argos secretion from cell *i*; this is modeled by a linear generation term in the equation for Argos. Separate linear processes describe the endocytosis of dimerized receptor and cell surface bound Argos, as well as the degradation of the intracellular transcription factor.

Since secreted Spitz has been identified as a limiting component in VE patterning (Chang et al., 2001, 2003; Schweitzer et al., 1995b), we assume that EGFR signaling in the VE operates in the ligand-limiting regime, meaning that the number of available receptors is not appreciably diminished by ligand binding. Thus, the receptor is in excess and the extent of its activation is controlled by the availability of secreted Spitz. Our previous analysis of EGFR activation by Spitz in cultured cells (and consideration of the human EGFR system) indicates that dissociation of EGFR-bound Spitz is slow compared to the rate of its internalization (Klein et al., 2004). We therefore assume that Spitz/EGFR binding is effectively irreversible on the

time scales relevant for pattern formation. Based on the biochemical analysis of Argos/Spitz interactions, we assume that Argos/Spitz binding is irreversible.[1] Finally, based on the fact that ligand-induced EGFR dimerization and phosphorylation is fast (Klein et al., 2004; Schweitzer et al., 1995b), we assume that it adjusts instantaneously to the levels of EGFR-bound Spitz at the cell surface.

With these assumptions, EGFR/Spitz/Argos signaling in the ventral ectoderm can be described in terms of three variables: P_i (t), the intracellular level of Pointed in cell i, and the extracellular concentrations of Argos ($A(x,t)$) and Spitz ($S(x,t)$) (see Supplementary Material for detailed derivation). For convenience, these variables are rescaled by their maximal concentrations (given by the balance of their generation and degradation, see Supplementary Material). After rescaling, the variables are denoted by p_i (t), $a(x,t)$, and $s(x,t)$. We choose the cell size as the unit of length (x).

Equations and parameters

Within the framework of our model, the steady state pattern of EGFR activation in the ventral ectoderm is described by the following boundary value problem (see Supplementary Material for details of model formulation and analysis):

$$\lambda_s^2 s_{xx} + f_s(x) - f_r(x)s - \mu as = 0 \quad (1)$$

$$\lambda_a^2 a_{xx} + f_a(\mathbf{p},x) - a - \nu as = 0 \quad (2)$$

Eqs. (1) and (2) describe the spatial profiles of secreted Spitz and Argos, respectively. The first term in these equations describes diffusion of secreted ligand (the second derivative with respective to the spatial coordinate multiplied by the corresponding length scale). The center of the midline cell is chosen as the origin, $x = 0$. No-flux boundary conditions are applied for s and a: $s_x|_{0,n} = 0$, $a_x|_{0,n} = 0$, where the size of the domain corresponds to n cells. The boldface $\mathbf{p}$ refers to the set of Pointed levels, p_i, for all cells i from zero to n.

The source function, $f_s(x)$, in Eq. (1) describes the pattern of Rhomboid expression, and hence the pattern of Spitz secretion. Rhomboid is expressed only in the midline cell; assuming symmetry around the midline, we therefore get $f_s(x) = 1$ when $x \leq 1/2$, and zero otherwise. The function $f_r(x)$ describes the localization of the EGF receptor (Raz and Shilo, 1993; Zak et al., 1990). The source function in the Argos balance Eq. (2), $f_a(\mathbf{p},x)$, describes the spatial pattern of Argos release, which is colocalized with the pattern of Pointed expression; for each cell, $f_a(\mathbf{p},x) = \text{const} = p_i$. Each of these functions is illustrated in Fig. 2.

We assume the amount of signal received by cell i is proportional to the total number of dimerized EGFR molecules in a cell. This signal, denoted by σ_i, is proportional to the integral of the free Spitz concentration over that cell, and thus $\sigma_i \equiv \int_{\text{cell } i} s(x)dx$ (see the Supplementary Material for derivation). We model the induction of Pointed by EGFR as a sharp switch: $p_i = 1$ when $\sigma_i > \theta_p$ and zero otherwise. This means that when the signal received by cell i (σ_i) is above the threshold level (θ_p), *pointed* will be expressed in that cell. This reflects the experimentally observed sharp domains of *pnt*, *otd*, and *aos* expression in response to the gradient of EGFR activation (Chang et al., 2001, 2003; Golembo et al., 1996a,b, 1999; Skeath, 1998; Wessells et al., 1999).

Solution of Eqs. (1) and (2) depends on five dimensionless parameters (Table 1). Each of these dimensionless parameters describes the relative importance of competing physical phenomena. λ_s, defined as the ratio of the diffusion length of Spitz to the length of a cell, describes the balance of Spitz diffusion and degradation. The length scale of Spitz has been proposed to be 3–4 cell diameters, and thus we restrict our parameter λ_s to values between one and ten (Freeman, 1994). λ_a is the length scale of Argos, analogous to λ_s and has been estimated to be 4–10 cell diameters (Freeman et al., 1992; Golembo et al., 1996b); we allow λ_a to vary between zero and ten. The parameter θ_p describes the threshold level of EGFR activity required for *pointed* expression. We constrain this parameter using experimental data from wild type embryos using the protocol described in the next section. The final two parameters, μ and ν, are related to Argos/Spitz binding. μ compares the kinetics of removal of free Spitz due to Argos/Spitz binding to the kinetics of Spitz degradation due to receptor binding and endocytosis. Analogous to this, ν is the ratio of removal rate of free Argos due to Argos/Spitz binding to the rate of Argos degradation associated with cell-surface binding. Based on surface plasmon resonance data (Klein et al., 2004), we estimate that μ is between 10^{-1} and 10^{1}, and ν, which is slightly less characterized, is between 10^{-2} and 10^{2} (see the Supplementary Material). These initial estimates are further refined by fitting experimental data in the aos^- mutant embryos.

Constraining the model parameters using experimental data from aos^- mutants

We use quantitative experimental data on EGFR-mediated gene expression in wild type and aos^- mutant embryos to constrain the parameters used in the model. Since the spatial domains of EGFR-target gene expression are sharp, we model target gene expression in any given cell using steep functions of the total number of EGFR

[1] In the Supplementary Material, we have also analyzed the limit when the equilibration of Argos/Spitz binding is infinitely fast. In this regime, Argos/Spitz binding is always in equilibrium. We have found that while this limit can describe the experimentally observed cell fate expansions in aos^- embryos, it does not lead to a robust patterning mechanism.

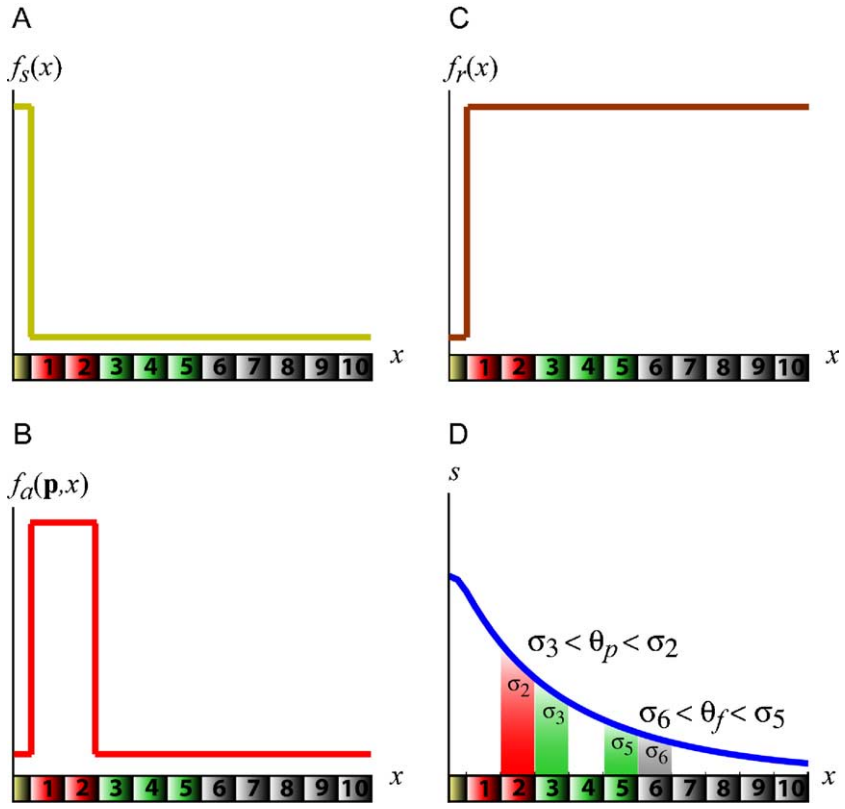

Fig. 2. Examples of model functions. (A) The function $f_s(x)$, denoting the expression pattern of secreted Spitz. Note that this function is equal to one above the midline cell and zero everywhere else, because Spitz is secreted by the midline cell only. (B) The function $f_a(\mathbf{p},x)$, denoting the *pointed*-dependent expression pattern of secreted Argos. Note that this function is equal to one above the cells expressing *pointed*, and zero everywhere else. (C) The function $f_r(x)$, denoting the expression pattern of EGFR. Note that this function is equal to one above the ventral ectodermal cells and zero over the midline cell. (D) Steady state Spitz concentration profile. The signal received by cell i is calculated by evaluating the integral under this curve above cell i. The thresholds are calculated based on the constraints described in the text.

dimers in that cell. We denote the threshold levels of Spitz (and thus of EGFR activity) required for *pnt*/*otd* and *fasIII* expression by θ_p and θ_f, respectively. Thus, $\sigma_i \geq \theta_p$ for *pnt*/*otd* expression in cell i; for *fasIII* expression we must have $\sigma_i \geq \theta_f$.

To determine whether our model can correctly predict the change in expression patterns of EGFR-target genes in *aos*$^-$ versus wild type embryos, we systematically sampled the parameters of the model (within the ranges described in the previous section) and tested their consistency with the reported *aos*$^-$ embryo data. To do this, we solved Eqs. (1) and (2) for each parameter set in the wild type case, assuming that Pointed is expressed in two cell rows on either side of the midline in wild type embryos (Chang et al., 2001, 2003; Golembo et al., 1996a,b). Next, we used the modeled Spitz profile to calculate σ_i for each cell. Since Pointed is expressed only in cells one and two of wild type embryos, and not in cell three, cell two must receive an EGFR signal that exceeds the threshold value θ_p, whereas cell three must receive a signal that is below θ_p (see Fig. 2D). This rule allowed us to estimate a value for θ_p in the wild type "embryo" characterized by a particular set of values for λ_s, λ_a, μ, and ν. We take θ_p to be the average between the signal received by cell two and the signal received by cell three: $\theta_p = (\sigma_2 + \sigma_3)/2$ (see Fig. 2D). Similarly, we take θ_f as $\theta_f = (\sigma_5 + \sigma_6)/2$. Once computed, the θ_p and θ_f values can be used to score whether or not a particular parameter set (λ_s, λ_a, μ, ν) is consistent with the experimentally observed expansion of EGFR-target gene expression domains in the *aos*$^-$ embryo. We scored a parameter set as "successful" if the model predicted both expansion of the *otd* domain to 4–6 cell rows, and expansion of the FasIII domain to 7 cell rows in the *aos*$^-$ mutant (see Figs. 3A, B).

From our calculations, we find that the model based on sequestration of activating ligand by Argos can successfully fit the literature data on cell fate expansions in the *aos*$^-$ mutant. Any length scale for Spitz (λ_s) between 1 and 10 can predict the correct patterning, although for $\lambda_s < 2$ the proportion of parameter space for which this is true is significantly reduced (see Fig. 3C). Contrary to the earlier argument that Argos is always a long-ranged diffusible inhibitor of EGFR signaling in *Drosophila*, based on clonal analysis experiments in the eye (Freeman et al., 1992), we find that the Argos length scale, λ_a, does not need to be larger than the length scale

Table 1
Model parameters

Parameter	Description
D_s	Effective diffusivity of Spitz
D_a	Effective diffusivity of Argos
k_s	Effective degradation of Spitz
k_a	Effective degradation of Argos
g_s	Rhomboid-derived generation of Spitz
g_a	Pointed-derived generation of Argos
k_{bind}	Binding rate constant between Argos and Spitz
L	Cell diameter
k_{ec}	Endocytosis rate of EGFR dimers
R_T	Threshold # of EGFR dimers for *pnt* expression

Parameter	Grouping	Value	Description
λ_s	$\frac{\sqrt{D_s/k_s}}{L}$	0–10	Length scale of Spitz
λ_a	$\frac{\sqrt{D_a/k_a}}{L}$	0–10	Length scale of Argos
μ	$\frac{k_{bind}g_a}{k_s k_a}$	10^{-1}–10^{1}	Removal rate of Spitz due to ligand sequestration
v	$\frac{k_{bind}g_s}{k_s k_a}$	10^{-2}–10^{2}	Removal rate of Argos due to ligand sequestration
θ_p	$\frac{k_{ec}R_T}{g_s L}$	–	Threshold signaling required for *pnt* expression

The first ten parameters are physical constants describing the properties of the system. The last five are dimensionless groups that arise from scaling the equations. Each dimensionless group compares two important physical properties of the system.

of Spitz, λ_s, in order to predict the observed alterations in EGFR-target gene expression patterns in *aos*$^-$ embryos; in fact, λ_a is not constrained at all (see Fig. 3D). Thus, in light of the recent biochemical demonstration that Argos inhibits EGFR signaling by sequestering diffusible ligand rather than blocking non-diffusible receptor, our model suggests a quite different interpretation for the range of Argos effects in the ventral ectoderm. Although the length scale of Argos may differ in distinct developmental contexts, in ventral ectoderm patterning Argos may in fact be a short-ranged molecule that remotely inhibits EGFR by preventing diffusible Spitz from reaching its intended destination.

Robustness of the EGFR-mediated patterning to altered gene dosages in wild type embryos

Having established that our model can successfully account for cell fate expansions in *aos*$^-$ embryos, we next assessed the robustness of the generated fits. This tests both the quality of the fits and the robustness of the underlying patterning mechanism. The Spitz gradient, and hence the gradient of EGFR activation, can in principle be altered by variations in the level of Spitz secretion from the midline cell. In addition, the level of EGF receptors in the ventral ectoderm may affect the morphogen gradient—even in the ligand limited regime—by a "ligand trapping" mechanism (Casanova and Struhl, 1993) that would become more prevalent for a given ligand-binding affinity as the number of receptors increased. By contrast with these expectations, however, experimental studies show that expression of EGFR-target genes is unchanged when the levels of Spitz secretion or receptor concentration are altered (Golembo et al., 1996a). How much of this robustness requires tight control of the amount of secreted morphogen and of the level of the cognate receptor? Alternatively, how much can be attributed solely to the structure of the extracellular signaling network and negative feedback by Argos? We have used our model to address these questions.

Let α_s and α_r denote the fold changes in the levels of Spitz secretion and EGFR expression, respectively, relative to the "average" wild type embryo for which $\alpha_s = \alpha_r = 1$. We randomly selected 300 of the parameter sets that were "successful" (as described above) in predicting expansion of EGFR-target gene expression domains in *aos*$^-$ embryos. For each parameter set, we used the model with wild type Argos to compute all possible combinations of α_s and α_r values for which the expression patterns of *otd* and *fasIII* remain identical to wild type. This revealed a series of robustness, or invariance, regions in the (α_s, α_r)-plane, inside which the wild type phenotype is maintained. An example of the invariance region calculated with $\lambda_s = 3.5$, $\lambda_a = 4$, $\mu = 2.25$, $v = 1$ is shown in Fig. 4A (rightmost gray region enclosed by blue curve). By measuring the widths of these invariance regions, we extracted the maximum and minimum fold-changes in Spitz levels that can be tolerated by the system (while holding EGFR levels constant at the wild type level). Similarly, we calculated the system's tolerance to changes in EGFR levels alone by measuring the heights of these regions. This analysis shows that the network can tolerate significant variations in the doses of Spitz and EGFR. For example, for the wild type case shown in Fig. 4A, the network can tolerate nearly a 20% increase or decrease in rate of Spitz secretion (horizontal arrows). Even larger perturbations in the EGFR levels are tolerated; the system retains wild type *otd* and *fasIII* expression patterns even when the EGFR level is increased to more than double the wild type level and is decreased to nearly half (vertical arrows). This level of robustness requires that Spitz sequestration by Argos is very efficient, i.e., that formation of the Argos/Spitz complex is essentially irreversible, consistent with the very slow off-rates observed in our surface plasmon resonance studies (Klein et al., 2004). We find that a model with fast, reversible, Argos/Spitz binding kinetics fails to produce an expression pattern that is robust to midline Spitz fluctuations (see Supplementary Material). Specifically, the wild-type patterns predicted by this "reversible" model could tolerate changes in EGFR levels or Spitz secretion rates of at most 5%.

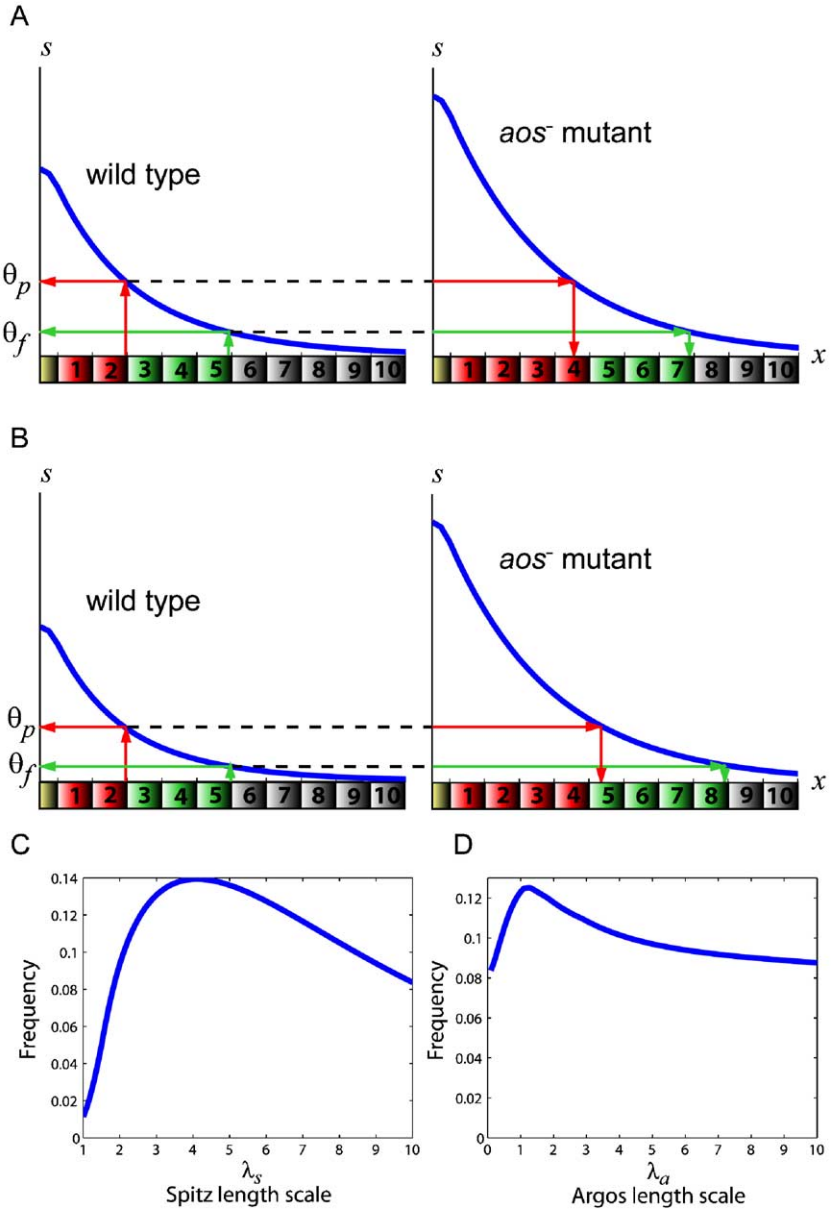

Fig. 3. Parameter screen based on *aos*$^-$ mutant data. (A, B) In wild type embryos, *otd* is expressed in two cell rows from the midline (red cells, left-hand panel), whereas FasIII is expressed in five cell rows (green and red cells, left-hand panel). We use the modeled Spitz profile to calculate σ_i, the amount of EGFR signal received by cell i. We then estimate the threshold signal level required for *pnt* (and hence *otd*) expression and denote this θ_p. Similarly, we calculate θ_f, the threshold signal level required for FasIII expression. We then use these threshold values to determine the predicted range of *otd* and FasIII expression in the *aos*$^-$ mutant (right-hand panel). (A) Calculation performed for a "successful" parameter set: $\lambda_s = 3$, $\lambda_a = 5$, $\mu = 3$, $\nu = 1$. Note that the expansions depicted in the Argos mutant are consistent with the literature data. (B) Calculation performed for an "unsuccessful" parameter set: $\lambda_s = 3$, $\lambda_a = 5$, $\mu = 5$, $\nu = 1$. Note that the expansions depicted in the Argos mutant here are inconsistent with the literature data. (C, D) Distributions of length scales for all parameter sets that are "successful" in fitting the *aos*$^-$ mutant data.

Within the randomly selected group of parameter sets tested, we next asked whether any correlation could be detected between any of the four dimensionless parameters shown in Table 1 and the maximum tolerated fold-changes in levels of EGFR and midline-derived Spitz. As shown in Figs. 4B, C, the maximal tolerated fold-changes were strongly correlated with the Spitz length scale, λ_s. This behavior is remarkable given that the maximal fold-changes were computed for a wide range of λ_s, λ_a, μ, and ν. None of the other dimensionless parameters showed any significant correlation with α_s or α_r, including the length scale of Argos (data not shown).

The computed boundaries for α_s and α_r can be used to quantify the robustness of the modeled system. The results shown in Fig. 4B illustrate that the system can tolerate midline fluctuations of up to 20% based solely on regulation at the level of Argos and the extracellular patterning network. Also shown in Fig. 4B is a significant decrease

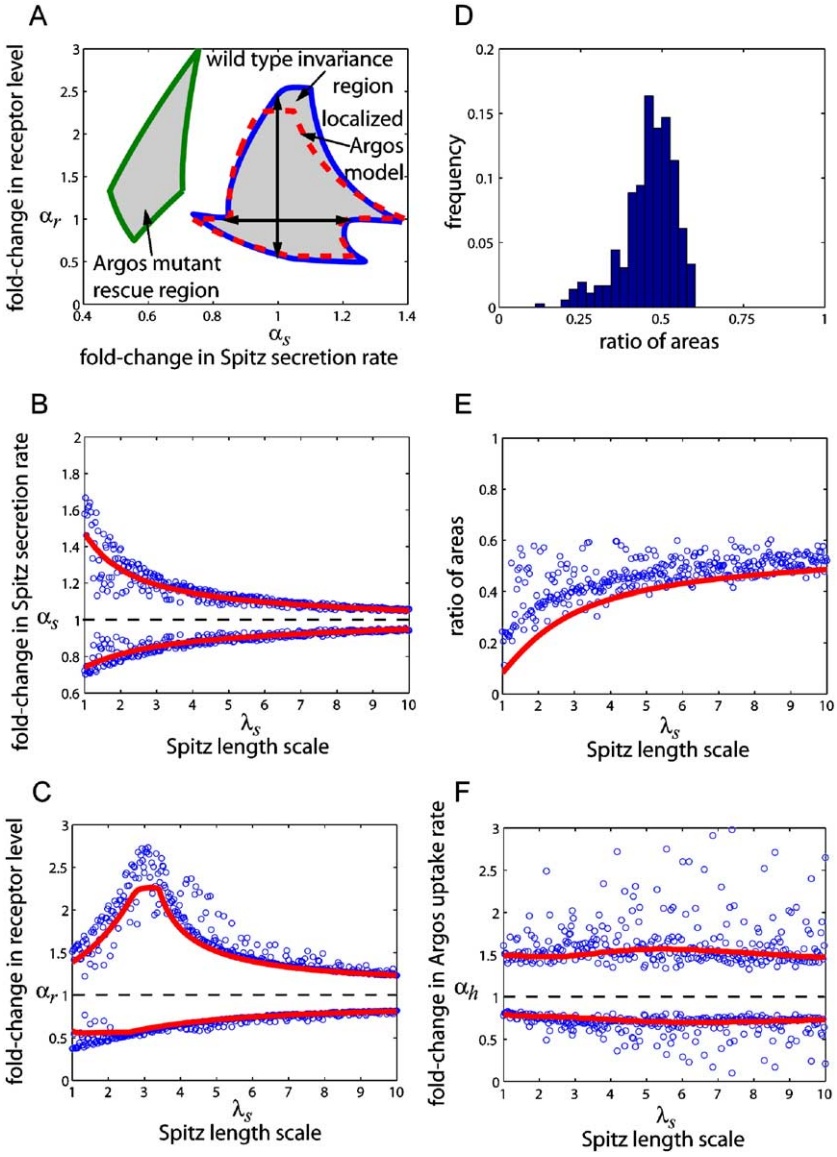

Fig. 4. Sensitivity of the patterning system to the levels of various components. (A) To determine the robustness of the system, we calculated the fold-changes in EGFR level (α_r) and Spitz secretion rate (α_s) that the system could tolerate while maintaining a wild-type expression pattern of both sets of marker genes. These constraints define a region in the (α_s, α_r)-plane that is depicted here for $\lambda_s = 3$, $\lambda_a = 4$, $\mu = 2.25$, $\nu = 1$ (rightmost gray region enclosed by solid blue curve). The dashed red curve denotes the corresponding region in the simplified model formulated with a localized, nondiffusible, Argos. The vertical and horizontal arrows indicate the maximal perturbations to α_r or α_s alone, respectively. The gray region enclosed by green curve shown to the left depicts the region in this plane where *aos*$^-$ mutant embryos will display the wild-type pattern of marker gene expression. (B, C) The maximal tolerated perturbations to the fold-changes in Spitz secretion rate (depicted as horizontal arrows in (A)) and the EGFR expression level (depicted as vertical arrows in (A)), for all randomly chosen parameter sets (blue circles), are plotted against the Spitz length scale. The solid red curves denote the corresponding maximal perturbations in the simplified model with localized Argos. (B) Maximal perturbations to fold-changes in the Spitz secretion rate. (C) Maximal perturbations to fold-changes in the EGFR level. (D, E) Analysis of the role of the negative feedback loop. The area of the region of Argos mutant rescue and the area of the corresponding wild type invariance region are compared. (D) Distribution of ratios of these areas found for 300 randomly generated parameter sets. Note that all ratios are significantly less than 1. (E) Plot of the ratio of these areas versus the Spitz length scale for the 300 randomly generated parameter sets (blue circles). The solid red curve denotes the same calculation performed with the simplified model with localized Argos. (F) The maximal tolerated perturbations to the fold-changes in Argos uptake rate for all randomly chosen parameter sets (blue circles), plotted against the Spitz length scale. The solid red curves denote the corresponding maximal perturbations in the model with localized Argos.

in robustness of the system with respect to changes in the Spitz dose (α_s) as λ_s increases. In contrast to the decreasing robustness with respect to changes in the Spitz dose as λ_s increases, we find that robustness to changes in EGFR levels (α_r) reaches a clear maximum when $\lambda_s = 3$ or 4 cell diameters (Fig. 4C), withstanding up to a 2 1/2 times increase and a 50% decrease. Again, this robustness is attributed solely to Argos action and to the inherent topology of the extracellular signaling module, and does not take into account other forms of regulation (so

represents a minimum estimate). Based on the peak in the robustness plot shown in Fig. 4C, we propose that the length scale of secreted Spitz, which is a function of its diffusion rate and rate of EGFR-mediated removal, must be 3–4 cells for maximum robustness; this is consistent with the length scale estimated from experiments in the eye imaginal disc (Freeman, 1994).

Robustness of the EGFR/Spitz/Argos network with respect to changes in the Spitz dose has been demonstrated previously in experimental studies. Increases in the dose of midline-derived Spitz do not affect the *otd* expression pattern (Golembo et al., 1996b). In addition, embryos heterozygous for a Spitz null mutation have a normal FasIII pattern (Golembo et al., 1999). Experiments in mutants with either reduced or elevated receptor levels have also shown no phenotypic effect on the spacing of the Keilin's organs precursors (Raz and Shilo, 1993). We have experimentally determined that this robustness can be traced to pattern formation in the VE. Indeed, the pattern of *otd* expression in the ventral ectoderm of stage 11 embryos from mutants with increased and decreased levels of EGFR was found to be indistinguishable from that in the wild type (see the EGFR gene dosage experiments described in Supplementary Material).

Contribution of Argos to robustness of EGFR-target gene expression patterns

The negative feedback provided by Argos is not required in order to achieve the observed wild type pattern of VE cell fates, which can readily be realized in an open-loop system without Argos, if the levels of Spitz secretion and/or EGFR expression are chosen appropriately. Instead, it has been suggested that one function of negative feedback signaling through Argos is to contribute to the observed robustness of VE patterning to perturbations in the EGFR/Spitz module, which is well described by our model (Golembo et al., 1996a). To test this hypothesis, we performed a mathematically controlled comparison (Alves and Savageau, 2000) between models of the wild type embryo and an Argos null mutant that was tuned to generate a wild type cell fate pattern. This analysis compares the robustness of the same steady state realized in two different patterning systems, the open-loop (Argos null) and the closed-loop (wild type).

We quantified changes in the sensitivity of the steady state gene expression pattern that result solely from removing the negative feedback loop through Argos by setting the negative feedback strength, μ (see Table 1 and Supplementary Material), to zero while holding constant as many other constraints as possible (including the length scale of Spitz and the two signaling thresholds). Removing the negative feedback loop in this way has drastic effects on the steady state pattern, making it impossible to simply compare the same steady state in both the wild type and Argos mutant cases. To overcome this difficulty we instead looked for the region in the (α_s, α_r)-plane in which the Argos mutant model predicts "rescue" of the wild type phenotype (Fig. 4A). We emphasize that, by construction, the wild type and mutant systems for each (wild type, mutant) pair evaluated in this manner have identical values for the thresholds of low- and high-threshold EGFR-target genes.

We found this region of Argos mutant rescue to be located to the left (lower values of α_s) of the corresponding invariance region for the wild type. This is natural, because rescue of an Argos mutant to wild type should involve lower levels of Spitz secretion to counteract the loss of the inhibitor. Next, to score the difference in sensitivities of the two systems, we computed the ratio of the area of the Argos mutant rescue region to the area of the invariance region for the corresponding wild type system. If the negative feedback loop (which we have removed) is instrumental in conferring robustness to the signaling module, the ratio of these areas should be significantly less than one, as is clearly the case in Fig. 4A. Repeating these calculations for a large range of parameters, we plotted the distribution of the ratio of these areas (Fig. 4D) for the randomly generated parameter sets defined as successful in Fig. 3. The area of the robustness region in the wild type embryo was always significantly greater than that of the Argos mutant rescue region. As in other measures of robustness, the ratio of these areas correlates well with the length scale of Spitz (Fig. 4E), with a trend towards increased robustness with decreasing Spitz length scale. Thus, our computational analysis argues that Argos contributes significantly to the robustness of the EGFR/Spitz/Argos signaling system, which can be tested explicitly in future experiments.

The histogram in Fig. 4D is constructed from all sets of parameters that pass the screen based on the Argos mutant data. We have also performed a more detailed analysis of the sensitivity of the ratio of robustness regions in the wild type and mutant models to the length scales of Argos and Spitz (results not shown). Specifically, we have found that the contribution of the negative feedback to robustness of the system is anticorrelated with the length scale of Spitz (and with the dynamic range in the model). By restricting this analysis to systems with a given dynamic range (that is tightly correlated with the length scale of Spitz, see Fig. S3 in the Supplementary material), we have found that the length scale of Argos essentially does not affect the contribution of the negative feedback to robustness of the EGFR-target gene expression patterns in the wild type system. Thus, our conclusion about the contribution of Argos to robustness of the wild-type patterns does not depend on the particular value of the Argos length scale.

Argos can achieve its effects on patterning and robustness by acting at a very short range

As described above, the computational analysis of our model showed that it can predict both the changes in EGFR

target gene expression in *aos*$^-$ embryos and the robustness of the system to varying Spitz and EGFR levels, regardless of the value employed for the Argos length scale (λ_a). Since λ_a can assume any value without altering our ability to model these behaviors, it can be zero. In this extreme case, Argos is modeled as a localized, nondiffusible inhibitor that sequesters Spitz and prevents its delivery to distant EGF receptors (Fig. 5A). In the context of VE patterning, a model of this sort is sufficient to describe the long-ranged inhibitory action of Argos. As shown in the Supplementary Material, in this regime, the number of free parameters in the model can be reduced from four to only two: the length scale of Spitz, λ_s, and the effective removal rate of Spitz by Argos, μ. The governing Eqs. (1)–(2) reduce to:

$$\lambda_s^2 s_{xx} + f_s(x) - s(f_r(x) + \mu f_a(\mathbf{p}, x)) = 0 \quad (3)$$

From this equation and the definition of the signaling thresholds (described above), we can compute the region of parameter space (λ_s,μ) that correctly predicts changes in EGFR target gene expression domains in *aos*$^-$ embryos. This region is plotted in Fig. 5B. We find that this simplified model provides a remarkably accurate approximation of the results generated by our full model. In particular, the variations in the Spitz and EGFR levels that are tolerated without changes in the *otd* and FasIII domains in this $\lambda_a = 0$ model agree very well with the results of the full, four-parameter model (see dashed red curve in Fig. 4A and solid red curves in Figs. 4B, C, E for representative examples).

In the model with short-ranged Argos ($\lambda_a = 0$), high levels of EGFR signaling close to the point of Spitz secretion induce the production of a nondiffusible inhibitor that acts as a localized ligand-sink. In this case, inhibition of EGFR signaling by Argos in the VE may be classified as "self-enhanced ligand degradation". This general mechanism was recently shown to be robust with respect to changes in the dose of secreted signal (Eldar et al., 2003). Indeed, essentially every pair of parameters consistent with the observed cell fate expansions in *aos*$^-$ embryos is robust in the sense that that it predicts a wild type model that can tolerate significant variations in the levels of EGFR and locally produced Spitz. Thus, a mechanism involving remote inhibition of EGFR by short-ranged Argos can fit the data from Argos null embryos and provides the basis for explaining the observed robustness with respect to changes in the level of locally produced signal and its ubiquitously expressed receptor.

Sensitivity of the model to cell surface binding (and uptake) of Argos

We have assumed in our model that Argos binding to the cell surface represents the primary mode of Argos removal/degradation from the ventral ectoderm. To ensure that this assumption does not impact our conclusions, it is important to determine how dependent are the predictions of the model on the parameters used to describe this uptake. We therefore tested the sensitivity of the wild type steady state pattern to variations in the level of cell surface Argos binding sites, and thus the Argos removal rate. Let α_h denote the fold change in the level of cell surface Argos binding sites, relative to the "average" wild-type embryo for which $\alpha_h = 1$. For the parameter sets identified as "successful" in predicting *otd* and *FasIII* expression patterns in *aos*$^-$ embryos, we computed the upper and lower limits of α_h for which the wild type expression patterns of *otd* and *FasIII* remain unchanged. We find that the network can tolerate more than a 20% decrease in Argos binding to the cell surface or an increase of at least 50%. This behavior is largely independent of particular values of the four model parameters (see Fig. 4F). We therefore conclude that our choice of parameters to describe this characteristic of Argos does not affect the qualitative conclusions of our modeling analysis.

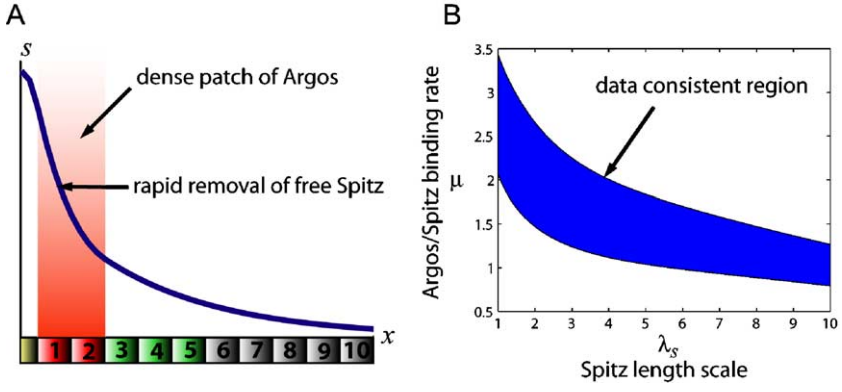

Fig. 5. Simplified model with immobile, localized, Argos. (A) Typical Spitz profile depicting the mode of action of localized Argos. Note the rapid decline in the Spitz profile in the region occupied by Argos. (B) Region of parameter space consistent with the *aos*$^-$ data.

Discussion

We have formulated a computational model for EGFR/Argos/Spitz interactions based on our recent biochemical demonstration that Argos interacts directly with Spitz, thus sequestering the ligand and preventing it from interacting with (and activating) *Drosophila* EGFR (Klein et al., 2004). We have used our model to analyze the patterning capabilities of this ligand-sequestration mechanism in EGFR-mediated cell fate determination in the ventral ectoderm. Our model can be directly correlated with the experimentally observed patterns of EGFR-target gene expression. We have reduced the number of free model parameters and developed a protocol for checking the consistency of any given parameter set with the published experimental data. Using this protocol, we find that the ligand sequestration mechanism for Argos action can successfully describe the experimentally observed cell fate expansions in *aos*$^{-}$ embryos. The model also predicts that the EGFR/Spitz/Argos patterning network can tolerate significant variations in the dose of Spitz and the level of EGFR expression—and is therefore robust—provided that the interaction between Argos and Spitz is significantly stronger than Spitz binding to EGFR, and is essentially irreversible. This predicted robustness has been tested and verified experimentally both in our own experiments (see Supplementary Material), and in previously published studies (Golembo et al., 1996b, 1999; Raz and Shilo, 1993). In addition, the requirement that Argos/Spitz binding is essentially irreversible is supported by the very slow dissociation of the complex seen in our surface plasmon resonance studies (Klein et al., 2004).

The robustness of the EGFR/Spitz/Argos network to variations in the Spitz dose indicates that precise patterns of EGFR-target gene expression in the ventral ectoderm do not require fine-tuning of Spitz production from the midline. Through our studies in both the wild type and Argos mutant networks, we find that this robustness is provided by negative feedback signaling through Argos. On average, our analysis indicates that the Argos mutant network is twice as sensitive (i.e., half as robust) as the wild type embryo to perturbations in both the Spitz dose and the receptor expression level.

Another important outcome of our analysis, summarized in Fig. 3C, is that Argos does not need to be long-ranged in order for the ligand sequestration mechanism to be consistent with available experimental data in VE patterning. We propose that, at least in the embryonic ventral ectoderm, Argos can remotely inhibit EGFR by acting only at very short range to sequester locally produced Spitz. This hypothesis is strongly supported by our demonstration that a reduced model, with non-diffusing Argos, quantitatively captures the behavior of the full mechanism over a wide range of parameter sets. The ultimate test of this prediction requires experimental visualization of Argos and Spitz gradients in the VE, and possibly efforts to manipulate Argos range experimentally.

Our model can be extended in a number of ways, and suggests several additional lines of experiments. First of all, the current formulation neglects Vein, a neuregulin-like EGFR ligand that is also induced by Spitz and is expressed in the same pattern as Argos (Chang et al., 2001; Golembo et al., 1999; Schnepp et al., 1996). Vein has been shown to play a role that is partially redundant with Spitz in VE patterning and appears to be required for maintaining the wild type domains of lateral EGFR-target gene expression when Spitz levels are compromised (Golembo et al., 1999; Schnepp et al., 1996; Skeath, 1998). Quantitative analysis of these effects in EGFR-mediated patterning requires future biochemical analysis of EGFR/Vein/Argos interactions, which are ongoing in our laboratories. A second important point is that our computational analysis of EGFR-mediated patterning has focused only on the final steady state pattern achieved in stage 11. The pathway to generation of this pattern is complex. The Spitz gradient in the naïve ventral ectoderm during stages 8–9 is established rapidly, and Argos is not initially present to modulate Spitz distribution. Thus, it could be argued that this developmental stage is analogous to an *aos*$^{-}$ mutant (since Argos expression has not yet been induced). Indeed, in stages 9–10 that follow, the domains of EGFR target gene expression are expanded compared with the stage 11 domains that we consider here (Gabay et al., 1996; Golembo et al., 1999). While our model agrees qualitatively with these observations and arguments (see Supplementary Material), future work should focus on the transcriptional network downstream of EGFR in these early stages, and how it is controlled. Specifically, the network of ETS transcription factors that include Pointed, Yan, and the auxiliary protein Mae has overlapping feedback loops that might contribute to the spatiotemporal regulation of EGFR activation in the ventral ectoderm (Vivekanand et al., 2004).

The computational analysis of EGFR inhibition by Argos presented here sheds light on the functional capabilities of control of receptor tyrosine kinases by secreted inhibitors. Our model shows that, by acting as a ligand-induced "ligand sink" produced close to the Spitz source (where Spitz levels are highest), Argos can act locally (at very short range) to restrict further Spitz signaling and/or to modulate the dose of Spitz delivered to distant cells. However, our model does not rule out the possibility that Argos can act at longer range, since neither robustness of the system nor the ability of our model to explain the available experimental data require that the Argos length scale is small. This raises the possibility that Argos might act over different ranges in distinct developmental contexts. For example, studies of the role of Argos in regulating cell fate decision in the *Drosophila* eye argue that it acts over several cell diameters (Freeman et al., 1992). The action of Argos as a ligand sink rather than a direct antagonist of the EGF receptor appears to lend this potential versatility to its function during development, and the studies presented here suggest future experiments and computational analyses to explore the

modes of EGFR regulation by Argos and other related ligand sinks in more detail.

Materials and methods

Fly strains

The following strains were used: Kr-Gal4 is a balanced double insertion on the third chromosome, directing expression in the Kruppel domain (segments T2-A4), UAS-EGFR-GFP and top^{IK35}/cyo a severe allele of the *top* gene (Clifford and Schupbach, 1994). All strains were kindly provided by T. Schüpbach.

In situ hybridization of whole-mount embryos

Otd cDNA plasmid was provided by T. Schupbach, and digoxigenin-labeled antisense RNA probe was prepared with Roche reagents. Embryos of top^{IK35}/cyo or from a cross between Kr-Gal4 and UAS-EGFR-GFP strains were collected for 2 h and aged for 5 h at 25°C (about stage 11), then hybridized with *otd* antisense RNA probe, as described (Gavis and Lehmann, 1992).

Acknowledgments

We thank Trudi Schüpbach, Cyrill Muratov Joseph Duffy, Diego Alvarado, Nir Yakoby, and members of the Lemmon and Shvartsman laboratories for many valuable discussions and for critical reading of the manuscript; Trudi Schüpbach for providing cDNAs and fly stocks. R.K. thanks Seema Chatterjee for help with setting up the experiments in the embryo. This work was supported by grants R01-CA079992 from the NIH (to M.A.L.) and NSF (S.Y.S.), by NIH training grant support and Predoctoral Fellowship BC030019 from the U.S. Army Breast Cancer Research Program (to D.E.K.), and by an NSF graduate research fellowship (G.T.R.).

Appendix A. Supplementary data

Supplementary data associated with this article can be found, in the online version, at doi:10.1016/j.ydbio.2005.05.013.

References

Alves, R., Savageau, M.A., 2000. Extending the method of mathematically controlled comparison to include numerical comparisons. Bionformatics 16, 786–798.

Casanova, J., Struhl, G., 1993. The torso receptor localizes as well as transduces the spatial signal specifying terminal body pattern in *Drosophila*. Nature 362, 152–155.

Casci, T., Freeman, M., 1999. Control of EGF receptor signalling: lessons from fruitflies. Cancer Metastasis Rev. 18, 181–201.

Chang, J., Kim, I.O., Ahn, J.S., Kim, E.S., 2001. The CNS midline cells control the spitz class and Egfr signaling genes to establish the proper cell fate of the *Drosophila* ventral neuroectoderm. Int. J. Dev. Biol. 45, 715–724.

Chang, J., Jeon, S.H., Kim, S.H., 2003. The hierarchical relationship among the spitz/Egfr signaling genes in cell fate determination in the *Drosophila* ventral neuroectoderm. Mol. Cells 15, 186–193.

Clifford, R., Schupbach, T., 1994. Molecular analysis of the *Drosophila* Egf receptor homolog reveals that several genetically defined classes of alleles cluster in subdomains of the receptor protein. Genetics 137, 531–550.

Colin, S., Jeanny, J.C., Mascarelli, F., Vienet, R., Al-Mahmood, S., Courtois, Y., Labarre, J., 1999. In vivo involvement of heparan sulfate proteoglycan in the bioavailability, internalization, and catabolism of exogenous basic fibroblast growth factor. Mol. Pharmacol. 55, 74–82.

Deguchi, Y., Okutsu, H., Okura, T., Yamada, S., Kimura, R., Yuge, T., Furukawa, A., Morimoto, K., Tachikawa, M., Ohtsuki, S., Hosoya, K., Terasaki, T., 2002. Internalization of basic fibroblast growth factor at the mouse blood–brain barrier involves perlecan, a heparan sulfate proteoglycan. J. Neurochem. 83, 381–389.

Eldar, A., Rosin, D., Shilo, B.Z., Barkai, N., 2003. Self-enhanced ligand degradation underlies robustness of morphogen gradients. Dev. Cell 5, 635–646.

Freeman, M., 1994. The spitz gene is required for photoreceptor determination in the *Drosophila* eye where it interacts with the Egf receptor. Mech. Dev. 48, 25–33.

Freeman, M., Klambt, C., Goodman, C.S., Rubin, G.M., 1992. The argos gene encodes a diffusible factor that regulates cell fate decisions in the *Drosophila* eye. Cell 69, 963–975.

Gabay, L., Scholz, H., Golembo, M., Klaes, A., Shilo, B.Z., Klambt, C., 1996. EGF receptor signaling induces pointed P1 transcription and inactivates Yan protein in the *Drosophila* embryonic ventral ectoderm. Development 122, 3355–3362.

Gavis, E.R., Lehmann, R., 1992. Localization of nanos RNA controls embryonic polarity. Cell 71, 301–313.

Golembo, M., Raz, E., Shilo, B.Z., 1996a. The *Drosophila* embryonic midline is the site of Spitz processing, and induces activation of the EGF receptor in the ventral ectoderm. Development 122, 3363–3370.

Golembo, M., Schweitzer, R., Freeman, M., Shilo, B.Z., 1996b. Argos transcription is induced by the *Drosophila* EGF receptor pathway to form an inhibitory feedback loop. Development 1996, 223–230.

Golembo, M., Yarnitzky, T., Volk, T., Shilo, B.Z., 1999. Vein expression is induced by the EGF receptor pathway to provide a positive feedback loop in patterning the *Drosophila* embryonic ventral ectoderm. Genes Dev. 13, 158–162.

Harris, R.C., Chung, E., Coffey, R.J., 2003. EGF receptor ligands. Exp. Cell Res. 284, 2–13.

Holbro, T., Hynes, N.E., 2004. ErbB receptors: directing key signaling networks throughout life. Annu. Rev. Pharmacol. Toxicol. 44, 195–217.

Kim, S.H., Crews, S.T., 1993. Influence of *Drosophila* ventral epidermal development by the CNS midline cells and spitz class genes. Development 118, 893–901.

Klein, D., Nappi, V.M., Reeves, G.T., Shvartsman, S.Y., Lemmon, M.A., 2004. Argos inhibits epidermal growth factor receptor signalling by ligand sequestration. Nature 430, 1040–1044.

Lee, C.M., Yu, D.S., Crews, S.T., Kim, S.H., 1999. The CNS midline cells and spitz class genes are required for proper patterning of *Drosophila* ventral neuroectoderm. Int. J. Dev. Biol. 43, 305–315.

Lee, J.R., Urban, S., Garvey, C.F., Freeman, M., 2001. Regulated intracellular ligand transport and proteolysis regulate EGF receptor activation in *Drosophila*. Cell 107, 161–171.

Moghal, N., Sternberg, P.W., 2003. The epidermal growth factor system in *Caenorhabditis elegans*. Exp. Cell Res. 284, 150–159.

Patel, N.H., Snow, P.M., Goodman, C.S., 1987. Characterization and

cloning of fasciclin III: a glycoprotein expressed on a subset of neurons and axon pathways in *Drosophila*. Cell 48, 975–988.

Raz, E., Shilo, B.Z., 1993. Establishment of ventral cell fates in the *Drosophila* embryonic ectoderm requires DER, the EGF receptor homolog. Genes Dev. 7, 1937–1948.

Schnepp, B., Grumbling, G.T.D., Simcox, A., 1996. Vein is a novel component in the *Drosophila* epidermal growth factor receptor pathway with similarity to the neuregulins. Genes Dev. 10, 2302–2313.

Schweitzer, R., Howes, R., Smith, R., Shilo, B.Z., Freeman, M., 1995. Inhibition of *Drosophila* EGF receptor activation by the secreted protein Argos. Nature 376, 699–702.

Schweitzer, R., Shaharabany, M., Seger, R., Shilo, B.Z., 1995. Secreted Spitz triggers the DER signaling pathway and is a limiting component in embryonic ventral ectoderm determination. Genes Dev. 9, 1518–1529.

Shilo, B.Z., 2003. Signaling by the *Drosophila* epidermal growth factor receptor pathway during development. Exp. Cell Res. 284, 140–149.

Skeath, J.B., 1998. The *Drosophila* EGF receptor controls the formation and specification of neuroblasts along the dorsal–ventral axis of the *Drosophila* embryo. Development 125, 3301–3312.

Sweeney, C., Carraway, K.L.r., 2004. Negative regulation of ErbB family receptor tyrosine kinases. Br. J. Cancer 90, 289–293.

Vivekanand, P., Tootle, T.L., Rebay, I., 2004. MAE, a dual regulator of the EGFR signaling pathway, is a target of the Ets transcription factors PNT and YAN. Mech. Dev. 121, 1469–1479.

Wessells, R., Grumbling, G., Donaldson, T., Wang, S., Simcox, A., 1999. Tissue-specific regulation of vein/EGF receptor signaling in *Drosophila*. Dev. Biol. 216, 243–259.

Zak, N.B., Wides, R.J., Schejter, E.D., Raz, E., Shilo, B.Z., 1990. Localization of the Der/Flb protein in embryos—Implications on the faint little ball lethal phenotype. Development 109, 865–874.